Mansoura Engineering Journal

Volume 48 | Issue 4 Article 4

2023

A Synthesized Dual-Polarized Planar Slotted Antenna Array for SAR Sensors

Ahmed E. Gohar
Researcher at Electronics and Communications Engineering Department, Mansoura University, Mansoura, Egypt, Ahmed.E.Goher@gmail.com

Haythem H. Abdullah
Professor at the Microwave Engineering Department, Electronics Research Institute (ERI), Cairo, Egypt.

Mohy El din Abo El-soud
Professor at the Electronics and Communications Engineering Department, Mansoura University, Mansoura, Egypt

ORIGINAL STUDY

A Synthesized Dual-polarized Planar Slotted Antenna Array for SAR Sensors

Ahmed E. Gohar [a,*], Haythem H. Abdullah [b], Mohy E.D. Abo El-Soud [a]

[a] Electronics and Communications Engineering Department, Mansoura University, Mansoura, Egypt
[b] The Microwave Engineering Department, Electronics Research Institute (ERI), Cairo, Egypt

Abstract

A synthetic aperture radar (SAR) sensor antenna is the main concern in this research work. The antenna specifications are settled according to the link budget of a project funded by the Egyptian Space Agency. The antenna should achieve a 30 dBi gain and an SLL of less than −27 dB with a low-profile and simple structure. The proposed antenna is an array of 16 × 18 planar elements that based on microstrip technology. The 16 × 18 antenna array consists of 16 linear antenna arrays of 18 elements each. Each element of the antenna array has two orthogonal slots with dual-polarization capability. To overcome the disadvantages of high loss on an extended feeding network, the column array is designed using a series feed technique. Also, to keep the design simple, a corporate feed is used to form the planar array. Synthesized excitations are used to enhance the SLL to −27.2 dB. Also, a novel feeding network is designed to easily produce the required field distributions. The proposed antenna has a broad bandwidth (5.2−5.4 GHz). Furthermore, the proposed design achieves good broadside dual linear polarization. The proposed antenna has a high gain, a smaller beamwidth, a compact size, a good SLL, and a wide bandwidth, all of which are important parameters in SAR antennas.

Keywords: Antenna array, MoM/GA, SAR antenna, Series feed, Slot antenna, Synthesized radiation pattern, Synthetic aperture radar, Unequal excitations

1. Introduction

The antenna is a critical component in the design of a SAR sensor. Numerous parameters must be considered when designing an antenna for SAR applications, including efficiency, gain, bandwidth, polarization, and beam width. These parameters should be monitored to ensure that they meet the system's requirements. Additionally, the size and cost of the antenna fabrication are critical parameters. Due to the limited available space on the satellite body, the antenna size is often restricted. The size of the satellite affects several parameters, such as the cost of launch, lifetime, power, data budget, and orbit parameters. A great deal of research has been published in the field of synthetic aperture antennas using various design techniques. Slot antennas, patch antennas, slotted waveguides, and substrate-integrated waveguides are all used to create efficient and reliable antenna arrays, each with its own set of advantages and disadvantages.

Several investigations have been presented in the design of antennas for SAR applications. In (Zhou et al., 2022), a wideband L- and X-band antenna for SAR applications is presented. To provide dual-band operation with a single aperture, the antenna employs a frequency-selective surface (FSS). The presented work has impedance bandwidths of 46% in the X-band and 21% in the L-band. However, only a single polarization can be produced with a gain of 20 dBi. The antenna's complexity is increased by its five layers, increasing fabrication and integration challenges. The presented work has an SLL of −14 dB, which is quite high for SAR applications.

In (Kashihara et al., 2023), an X-band circularly polarized UAV-SAR is presented. By implementing another antenna, the presented work can produce a

Received 1 January 2023; revised 8 April 2023; accepted 13 May 2023.
Available online 12 July 2023

* Corresponding author.
E-mail addresses: ahmed.e.goher@gmail.com, ahmed.gohar@egsa.gov.eg (A.E. Gohar).

https://doi.org/10.58491/2735-4202.3052

dual polarization, which increases the antenna's dimensions. The antenna has an SLL and HPBW of −13 dB and 15°, respectively, in both planes. The antenna is suitable for UAV applications due to its wide beam width.

In (Yu et al., 2020), a 6 × 12 patch array is presented for millimeter-wave SAR applications. The patch sub-arrays are made up of 12-patch series-fed patch sub-arrays. A substrate-integrated waveguide feeding network is used to connect the sub-arrays. By feeding the series-fed linear arrays with a SIW corporate feeding network, the presented work introduces the concept of combining the series and corporate feeding networks. The combination of feeding network techniques reduces the design's complexity. To distribute the wave to the first substrate, the antenna uses two substrates, one for the series-fed patches and the other for the SIW feeding network. However, using multiple substrates increases the antenna's complexity, making it more susceptible to fabrication and integration errors and adding more losses due to wave leakage between substrates. The antenna can only produce a linear polarization with a wide beam width. The range and azimuth beam widths of the antenna are 15° and 9°, respectively. The work presented here has an SLL of −15 dB and a gain of 20.4 dBi.

In (Santosa et al., 2021), a circularly polarized microstrip array antenna with a broadband frequency range is introduced for SAR sensors. The antenna comprises an 8 × 8 array with a uniform element spacing of 0.5λ and uses a corporate proximity-coupled strip-line feeding network. The antenna generates circularly polarized waves by using a curved truncation patch and a circle-slotted parasitic patch above it, resulting in a wide bandwidth. The antenna can produce dual-polarized radiation, but it requires two separate antennas, which increases the overall antenna structure. The antenna produces a gain of 18.17 dBic, with an SLL of −8 dB and −11.9 dB in the azimuth and range planes, respectively, and an HPBW of 12.7° in the azimuth plane and 13° in the elevation plane. However, the antenna's complexity is increased by using a corporate feeding network implemented in another layer attached underneath the parasitic patch layer, making the overall antenna design more complex.

In (Qin et al., 2016), a dual-band, dual-polarized antenna with high gain for SAR applications is discussed. The antenna is designed based on the concept of a Fabry-Perot resonant cavity to achieve dual-band operation. The antenna can achieve a beam scanning angle range of ±15° in two orthogonal polarizations. The design employs two FSS layers to form two separate resonant cavities, providing high flexibility in selecting desired frequencies for each band. However, the use of multiple FSS layers increases the complexity of the design. The antenna has an SLL of less than −14.5 dB in both the azimuth and elevation planes at 5.3 GHz and a gain of 16.4 dBi with an HPBW of 28° in both planes. The antenna can produce dual-polarization radiation, but with a high SLL, large HPBW, and low gain.

In (Ravindra et al., 2017), a parallel-plate antenna array for SAR application on a small-satellite platform is presented. The antenna operates in the X-band frequency range and covers a bandwidth of 130 MHz with a center frequency of 9.65 GHz. The antenna presented can generate dual circular polarization with a beamwidth of 2.4° in both the azimuth and elevation directions. The gain is 34.5 dBic, and the SLL is −15 dB in the range and −11 dB in the azimuth directions, respectively. The antenna has a high gain and a narrow beamwidth, but it does so by utilizing a complicated waveguide and parallel-plate structures.

The contribution of this research work can be summarized as follows:

(1) The design is considered a generic design to introduce an antenna with an arbitrary beam shape.
(2) The design that should be implemented using either a complex planar structure or a 3D waveguide structure is implemented using only a simple single-layer structure.
(3) The challenges in implementing large dynamic range ratios in the synthesized feeding network are already solved by a proposed novel procedure for distributing the feeding power. Furthermore, the consequences of the proposed procedure, such as the nonlinear phase shift between ports, are also treated.

This paper proposes a dual-polarized orthogonal slot planar antenna array for SAR satellites, which consists of 16 × 18 elements. To increase efficiency and gain and to reduce design complexity, a series feed technique is employed to connect 18 dual-polarized elements in a linear array. A corporate feeding network with 16 output ports is merged with the series feeding network to form the planar array. The corporate feeding network is printed on the same antenna substrate to achieve a low-profile design and to reduce losses due to wave transfer between different substrates. Additionally, this design approach enhances reliability and reduces sensitivity to manufacturing errors. Two corporate feeding networks are utilized to provide dual

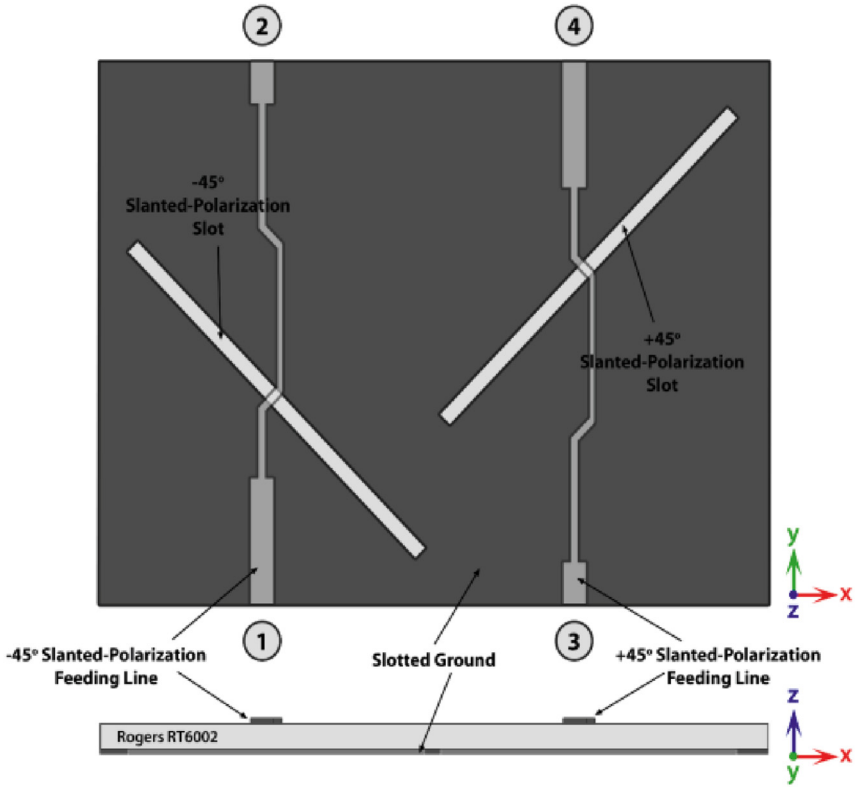

Fig. 1. The general view of the dual-polarized series-fed printed slot antenna element.

polarization radiation, with one placed at the bottom to excite the -45° slanted polarization and the other at the top to excite the $+45^{\circ}$ slanted polarization. To enhance image resolution, the antenna SLL must be controlled. The corporate feeding network is designed to produce a synthesized field disruption to linear arrays, providing a low side lobe level. Finally, a novel feeding network is designed to deliver the required excitations to the antenna elements with applicable dividing ratios. The design process involves four stages, including series element design, termination element design, column array design, and forming the planar array.

2. Antenna design

The proposed antenna is built by designing single elements that are then combined to form the overall antenna array. The linear array is made up of two types of single elements: series elements and

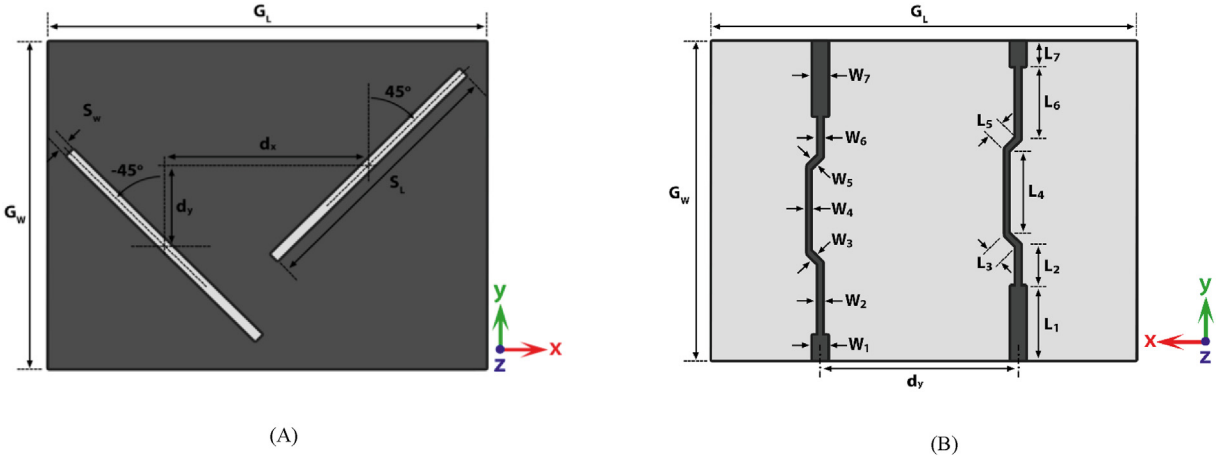

Fig. 2. The detailed dimensions of the series element, (A) Front view, (B) Back View.

Table 1. The dimensions of the series element.

Parameter	Value (mm)	Parameter	Value (mm)
S_L	31.5	S_w	1
d_y	9.66	G_L	52
L_1	9	W_1	1.8
W_2	0.5	L_3	2
L_4	10.88	W_4	0.3
W_5	0.4	L_6	9
L_7	3	W_7	1.8
d_x	23.19	W_3	0.4
G_W	39.5	L_5	2
L_2	5	W_6	0.5

termination elements. A series element is a type of element that is repeated in a chain to form a linear array. The last element in the linear array is the termination element. The series-fed arrays are used for designing the linear array as they can provide a good radiation pattern with a simple feeding network structure, which is needed in our work. Also, the series-fed arrays have been demonstrated to be an effective configuration for increasing antenna efficiency because the length of feedline runs is significantly reduced compared to the conventional tournament feed system (Metzler, 1981). Finally, a synthesized feeding network is designed to connect the linear arrays to form the planner array. The subsections that follow describe the steps of the antenna design.

2.1. Single element

As previously discussed, the proposed antenna design is divided into two main parts: the series element and the termination element. The design concept of the two elements is approximately the same. The elements consist of two perpendicular slots etched on the ground plane (Li et al., 2011), and two series microstrip feed lines are printed on the opposite plane of the antenna element. The series antenna element's general view is shown in Fig. 1, which shows the position of the slots relative to the feeding lines and describes the port numbers. Using two etched ±45° slanted slots, two orthogonal radiating modes are excited at the antenna's resonant frequency. This geometry allows radiating in two orthogonal polarizations.

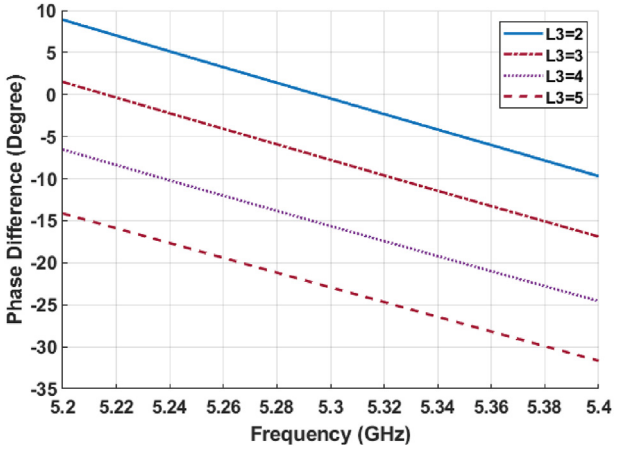

Fig. 3. The effect of L3 length on the phase.

To achieve maximum coupling, the feeding lines cross the etched slots with sloping line sections perpendicular to the etched slot (Vallecchi and Gentili, 2005). To improve radiation efficiency, step impedance matching is used to match the impedances between the slot and the microstrip line (Wang and Chen, 2014). To achieve the traveling-wave mechanism, each section of the antenna is impedance-matched to the feed line impedance (Pozar and Schaubert, 1993). All ports have a 50 Ω impedance termination. The input ports for the two slanted slots are ports 1 and 4. Fig. 2 and Table 1 show the dimensions of the series element. To change the phase of the transmission coefficient, the length of the feeding line sections can be stretched or decreased (Vallecchi and Gentili, 2005). The phase between two subsequent elements can be adjusted using this approach without changing the distance between them by modifying the length of L_3. Fig. 3 shows the effect of modifying the length L_3 on the phase difference between the input and output ports of one element. The feeding line's length and width are chosen to provide the necessary impedance matching as well as in-phase characteristics between the successive elements.

To provide good radiation efficiency, the series elements should be terminated by a matched load (Vallecchi and Gentili, 2005). The terminating antenna element, shown in Fig. 4, has the same structure as the series antenna element, but the feed lines have been altered to serve as a matched load. To get a 50 Ω impedance match, the slot and stub lengths are modified. The termination element is designed to emit radiation at the same center frequency as the series element, which is 5.3 GHz. The termination element is designed such that only one port is terminated, and the other port acts as the series element. By using this technique, the linear array can be fed from two opposite directions. Each feeding line is responsible for a single-slanted polarization. This simplifies the planar antenna array design by allowing the feeding network to be positioned on the same antenna layer on both sides of the antenna array. The concept of planar antenna design is introduced in the following section. Two termination elements are designed, and the linear

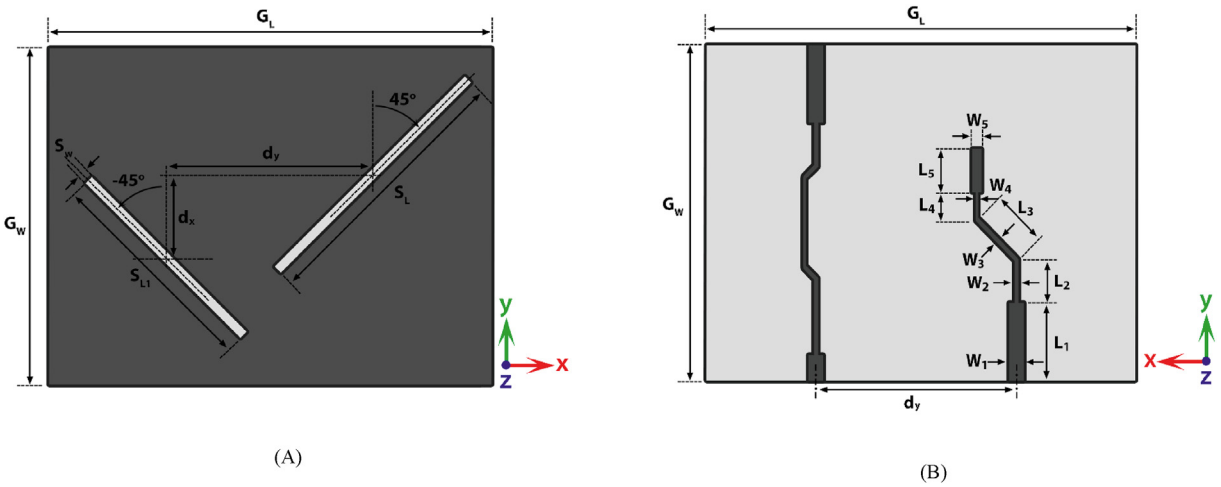

Fig. 4. The detailed dimensions of the termination element, (A) Front view, (B) Back View.

array is terminated by one element from the top and the other element from the bottom. The design principle for the two elements is the same, with a few modifications to match the slot direction. Table 2 shows the dimensions of the termination element.

2.2. Single column antenna array

The series antenna elements are cascaded to produce a linear antenna array as shown in Fig. 5. The column antenna array is terminated from both sides by the termination elements. The separation between two successive elements (d) is equal to $0.69\lambda_o = 39.5$ mm (λ_o is the wavelength at the operating frequency of $f_o = 5.3$ GHz). The linear array consists of 18 series elements and 2 termination elements. The overall dimension of the column is about 78.9×5.2 cm^2. The input port for the $+45^\circ$ slanted polarization is at the top of the array, and the other polarization is at the bottom of the array.

2.3. Synthesized planar antenna array

To shape the radiation pattern, an antenna radiation pattern synthesis algorithm is used. The algorithm is based on a combination of the MoM (Harrington, 1993) and the GA (Haupt and Werner, 2010; Rahmat-Samii and Michielssen, 1999). The algorithm reduces several elements using uniform or non-uniform element spacing. The MoM provides a deterministic solution for the excitation coefficients. On the other hand, the GA is used to estimate the optimum element locations to obtain the required radiation pattern within a minimum tolerance. As described in (Hussein et al., 2011), the Hybrid MoM/GA algorithm is applied to the synthesis of both symmetric and asymmetric radiation pattern distributions with a minimum number of elements. Also in (Eldosouky et al., 2013), a combination of the Fourier transform, curve fitting, and the genetic algorithm synthesizes linear arrays. This approach produces the required radiation shape using a minimum number of antenna elements by producing the optimum spacing and excitations of the antenna array elements. Table 3 shows the generated excitations from the MoM/GA algorithm.

As depicted in Table 3, the algorithm is used to produce symmetric and unequal field distributions across the antenna elements. The planar antenna uses the corporate feeding technique to feed the complete antenna (Riyazuddin and Bharath, 2015). The Wilkinson power divider is used as the main element in the feeding network (Lv et al., 2015). The planar antenna array is designed by repeating the single-column array in the x-direction and connecting it with Wilkinson power dividers. The power dividers are designed to deliver in-phase excitation with unequal power for the antenna array elements. The power ratio shown in Table 3 describes the required power that should be applied to each linear array. In order to design a feeding

Table 2. The dimensions of the Termination element.

Parameter	Value (mm)	Parameter	Value (mm)
S_L	31.5	S_w	1
d_x	23.19	d_y	9.66
G_W	39.5	L_1	9
L_2	5	W_2	0.5
W_3	0.4	L_4	3
L_5	5	W_5	1
S_L	31.5	L_3	7
G_L	52	W_4	0.3
W_1	1.8		

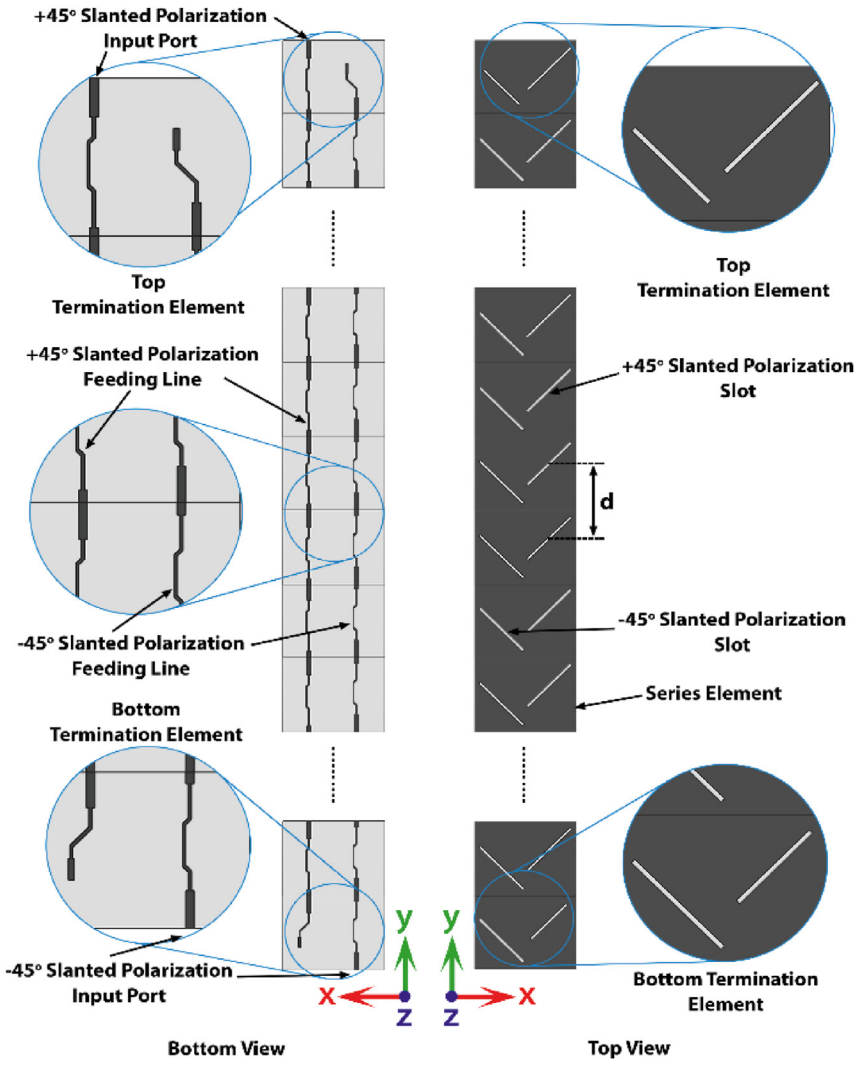

Fig. 5. Antenna single column design.

Table 3. The required excitations for each antenna array element.

Element number	Excitations	Power ratio
*P*2	0.1121	1.34%
*P*3	0.1581	1.88%
*P*4	0.2922	3.48%
*P*5	0.4557	5.43%
*P*6	0.503	5.99%
*P*7	0.7574	9.03%
*P*8	0.9169	10.93%
*P*9	1	11.92%
*P*10	1	11.92%
*P*11	0.9169	10.93%
*P*12	0.7574	9.03%
*P*13	0.503	5.99%
*P*14	0.4557	5.43%
*P*15	0.2922	3.48%
*P*16	0.1581	1.88%
*P*17	0.1121	1.34%

network to deliver the antenna elements with the required excitations according to Table 3, two proposed feeding distributions are shown in Figs. 6 and 7. The distribution in Fig. 6 is less complex in its design due to the equal wave paths from the main feeding port to the targeted output ports, which result in equal phases at the output port as required from the excitation coefficients in Table 3. But unfortunately, this configuration results in a power division ratio of 24%–76% between the two branches of some power dividers. This results in an unrealizable transmission line width in the low-power branches. The solution to this problem is to follow the distribution shown in Fig. 7. Fig. 7 illustrates the second proposed feeding network used to excite the linear antenna array.

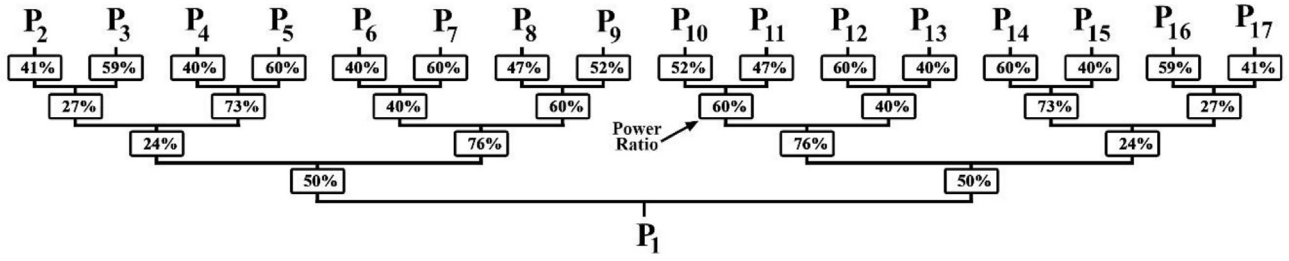

Fig. 6. The conventional feeding distribution network.

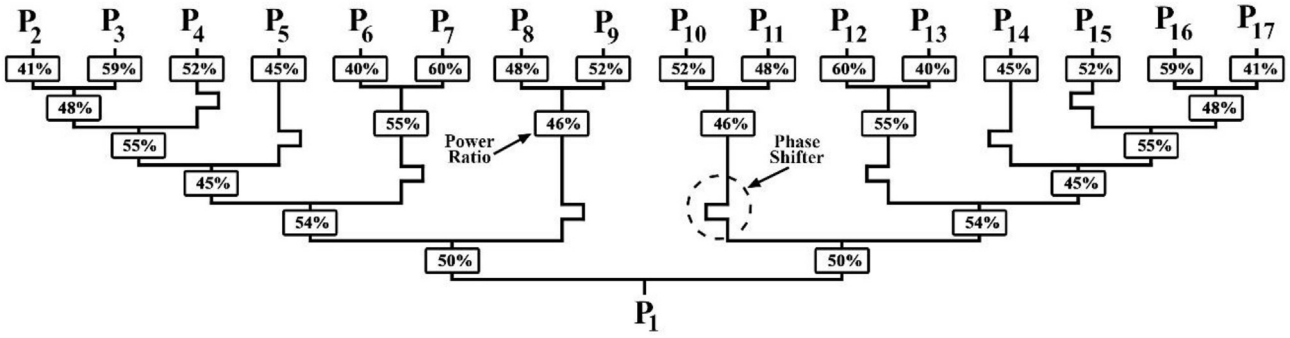

Fig. 7. The proposed design of the feeding network.

The proposed feeding network differs from the conventional one in that it significantly reduces dividing ratios, which can be efficiently designed and fabricated. The drawback of this structure is that it suffers from a phase difference between the output ports. It's required to drive the antenna element in phase to get the required far-field radiation pattern. To overcome this problem, a meander line is used as a phase shifter, which is placed on some power dividers' arms to compensate for the phase difference between the output ports. This structure provides in-phase excitations with the required field distribution for each column. The feeding network consists of 15 Wilkinson power dividers. The delivered power at each output port of the feeding network for the symmetric and the proposed distributions are shown in Tables 4 and 5), respectively. The tables show that both feeding distributions can supply the required power for each antenna element, but the proposed design has more designable ratios.

Table 4. The required Wilkinson power divider ratios at each stage for the conventional design.

	Dividing ratio at each stage				Delivered Power (%)
	S1	S2	S3	S4	
P2			0.27	0.41	1.33
P3		0.24		0.59	1.91
P4			0.73	0.4	3.50
P5	0.5			0.6	5.26
P6			0.4	0.4	6.08
P7		0.76		0.6	9.12
P8			0.6	0.47	10.72
P9				0.52	11.86
P10			0.6	0.52	11.86
P11		0.76		0.47	10.72
P12			0.4	0.6	9.12
P13	0.5			0.4	6.08
P14			0.73	0.6	5.26
P15		0.24		0.4	3.50
P16			0.27	0.59	1.91
P17				0.41	1.33

Table 5. The required Wilkinson power divider ratios at each stage for the proposed design.

	Dividing ratio at each stage						Delivered Power (%)
	S1	S2	S3	S4	S5	S6	
P2					0.48	0.41	1.32
P3				0.55		0.59	1.89
P4			0.45		0.52	–	3.47
P5		0.54		0.45	–	–	5.47
P6	0.5			0.4	–	–	5.94
P7			0.55	0.6	–	–	8.91
P8		0.46	0.48	–	–	–	11.04
P9			0.52	–	–	–	11.96
P10		0.46	0.52	–	–	–	11.96
P11			0.48	–	–	–	11.04
P12				0.6	–	–	8.91
P13	0.5		0.55	0.4	–	–	5.94
P14		0.54		0.45	–	–	5.47
P15			0.45		0.52	–	3.47
P16				0.55		0.59	1.89
P17					0.48	0.41	1.32

The distance between each output port is designed to be 52 mm, which equals $0.9\lambda_0$. The feeding network is designed on the same substrate as the antenna elements, as it will be impeded on the same substrate as the complete antenna (Li et al., 2014). Fig. 8 shows the planar antenna array design. The antenna array consists of 16 linear arrays connected by a tournament feeding network. Two feeding networks are used to provide dual-polarization radiation. One is placed at the bottom, which is used to excite the -45° slanted polarization. The other one excites the $+45^\circ$ slanted polarization. The total size of the array is $832 \times 789 \times 0.7972\ mm^3$. A reflector is placed in $\lambda_0/4$ which equals 15.7 mm, to provide the required directive radiation (Bayderkhani and Hassani, 2010; Weily and Guo, 2009).

3. Results and discussion

The proposed antenna is simulated using the Computer Simulation Technology (CST) software on Rogers RT6002 substrate material with a dielectric constant of $\epsilon_r = 2.94$, substrate height

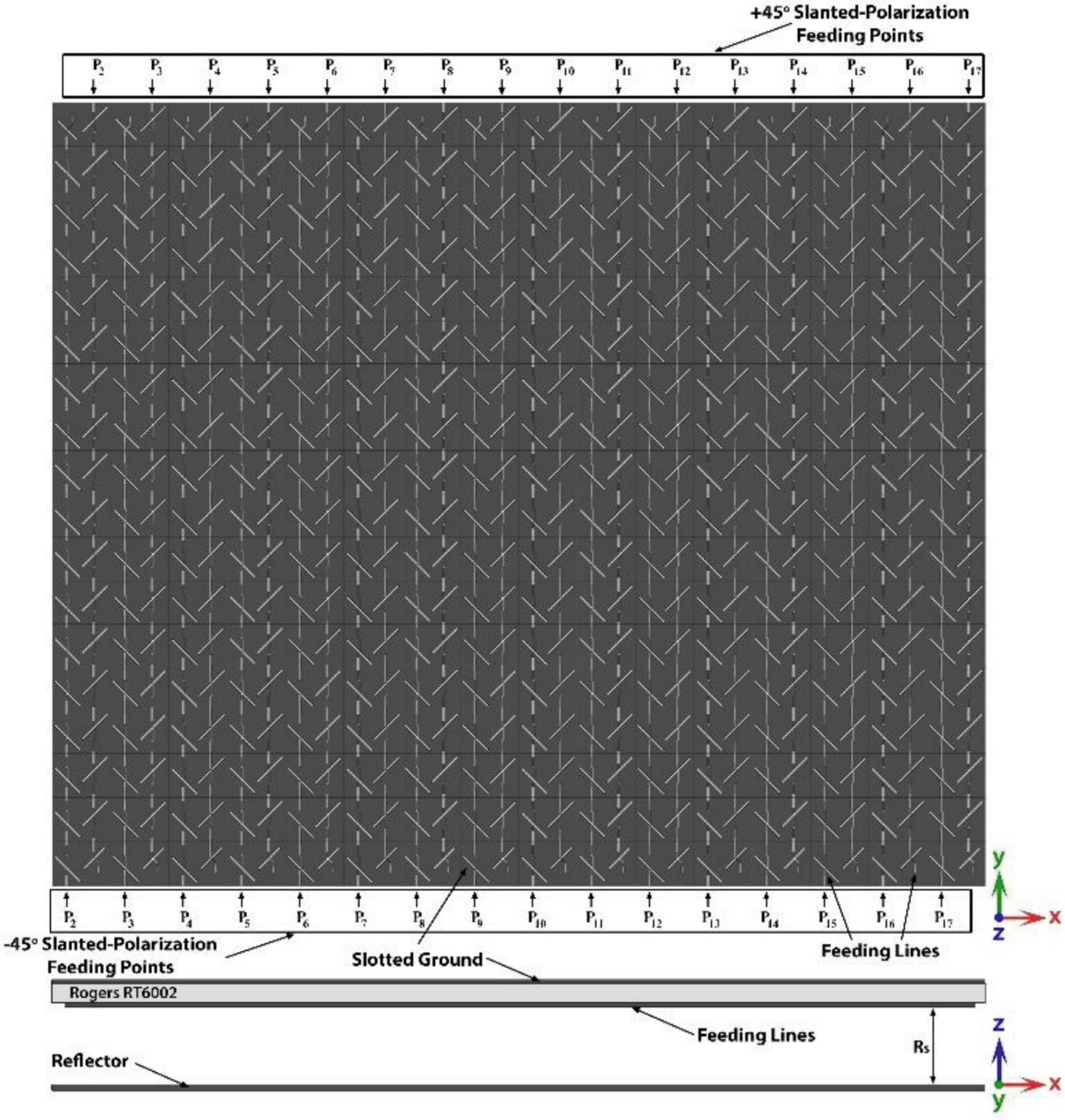

Fig. 8. The design of the proposed orthogonal-slots series-fed dual-polarized antenna array.

(h) = 0.762 mm, and loss tangent of 0.0012. RT6002 has been considered a substrate material because of its high reliability characteristics for aerospace applications (Corporation R). The results of the series element, termination element, linear array, and planar antenna array are presented and discussed in this section.

3.1. Single element

The results of the series element and termination element are discussed in this section. The series antenna element has four ports. Port 1 and port 4 are used as input ports for the dual-polarized antenna. Port 2 and port 3 are terminated with 50 Ω to match the series element impedance to the feed line impedance. On the other hand, the termination antenna element has only 3 ports. This element is used to terminate one polarization and pass the other one. The simulated reflection coefficients $|S_{11}|$ and $|S_{44}|$, the transmission coefficients $|S_{21}|$ and $|S_{34}|$, and the isolation coefficients $|S_{31}|$ and $|S_{41}|$, of the dual-polarized series antenna element are shown in Fig. 9a. The S-parameters of the series element show that the reflection coefficients are below −18 dB across all the required bandwidth, and the transmitted wave from one element to the next is above −2 dB. That's due to the good matching provided by the stepped impedance added to the feeding lines between the feeding line and the 50 Ω termination port.

Also, the simulated S-parameters of the termination element are shown in Fig. 9b. The reflection coefficient for the section that is utilized as a series element is represented as $|S_{11}|$. This section's transmission coefficient is given as $|S_{21}|$, and its value is −2 dB. The reflection coefficient of the termination section is represented by the $|S_{44}|$ and the isolation coefficient is described by $|S_{41}|$. The stepped transmission line that is added to the termination section makes the $|S_{44}|$ under −10 dB across the required bandwidth. As shown in the figures, both proposed antenna elements cover the required operational bandwidth (200 MHz), which ranges from 5.2 GHz to 5.4 GHz.

The radiation patterns of the series antenna element in −45° slanted polarization and +45° slanted polarization are shown in Fig. 10. The figures show that the main lobe magnitude is at 7.5 dBi, according to the figures. In addition, the figures depict the effect of a broadside reflector mounted behind the antenna. Also, the radiation patterns of the termination antenna element are shown in Fig. 11, which also provides the same gain as the series element.

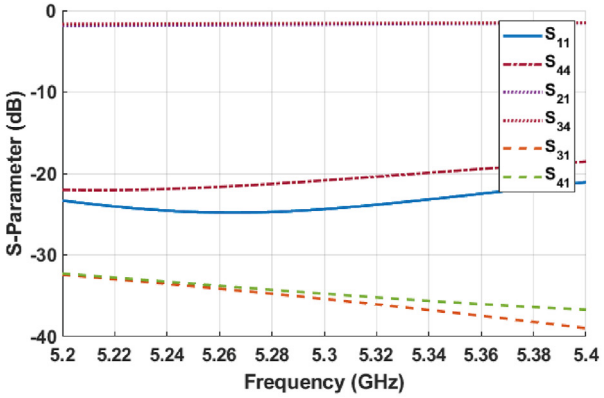

(a)

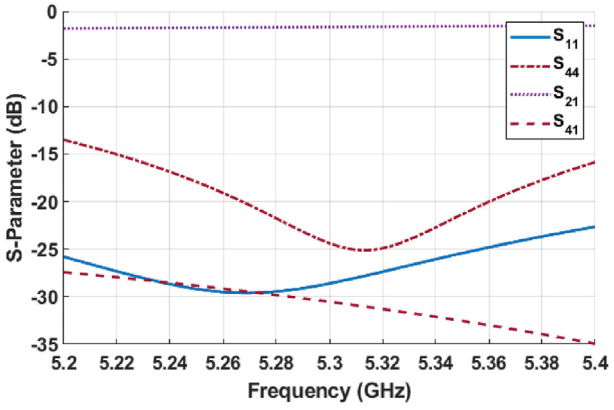

(b)

Fig. 9. The simulated S-parameter results of (a) series element and (b) termination element.

3.2. Column antenna array

This section presents the simulated results of the column antenna array. The simulated reflection coefficients $|S_{11}|$ and $|S_{44}|$ for the two orthogonal polarization inputs as well as the isolation coefficients $|S_{41}|$ and $|S_{14}|$ between the two inputs are shown in Fig. 12. The combination between the series elements and termination elements that are matched at the same resonant frequency, 5.3 GHz, makes the column antenna array cover the required operational bandwidth. The figure shows that the antenna covers a range of frequencies extending from 5.2 to 5.4 GHz. The use of a low-loss substrate improves the radiation characteristics of the antenna, which reflects on the gain of the column array. Fig. 13 shows the gain versus frequency, where it can be noted that the gain of the column antenna array is greater than 15 dBi within the required operating bandwidth. Fig. 14 depicts the polar radiation pattern in the −45° slanted and +45° slanted

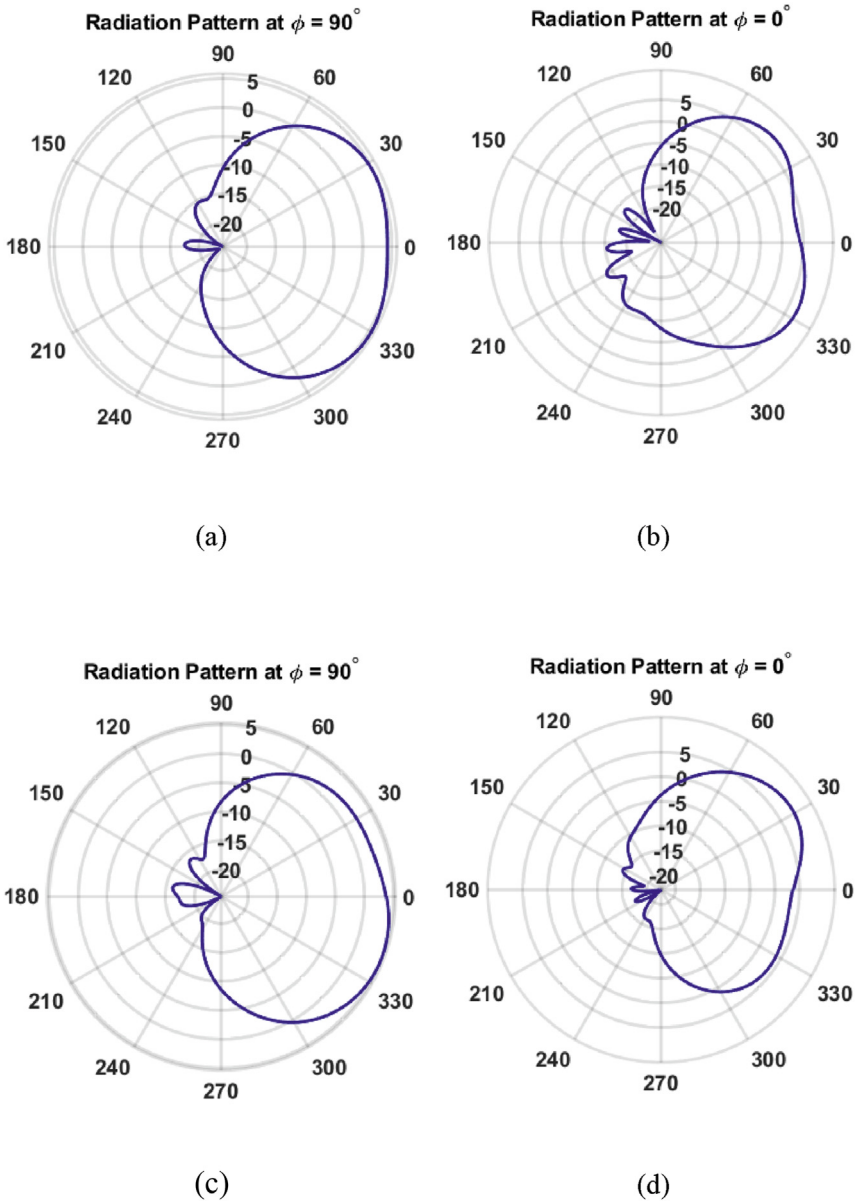

Fig. 10. The simulated radiation pattern of the dual-polarized series element at 5.3 GHz. (a) −45 slanted polarization at phi = 90°, (b) −45 slanted polarization at phi = 0°, (c) +45 slanted polarization at phi = 90° (d) +45 slanted polarization at phi = 0°.

polarizations. The figure shows that the beamwidth in the range direction is approximately 4.2°.

3.3. Planar antenna array

This section compares the equal distribution and the synthesized distribution planar array designs. The planar array is simulated using the array factor option in CST. First, the number of elements is selected to be 16 with an equal distribution. As shown in Fig. 15, the SLL is −12.7 dB and the HPBW is 3.5°. As described above, the MoM/GA algorithm is used to optimize the SLL.

The new synthesized distribution is used to simulate the antenna array. The figure also shows that the synthesized distributions enhance the SLL for the same number of elements. The new array produces an SLL of −27.2 dB with an HPBW equal to 5.1°. The radiation pattern output in polar coordinates is shown in Fig. 16. It can be noted that the range beamwidth is about 4.2°, as it is the same as the column array. The simulated gain of the antenna array is about 30 dBi for both polarizations.

Table 6 summarizes the performance of the proposed synthesized orthogonal-slots series-fed dual-polarized SAR antenna array with previous works.

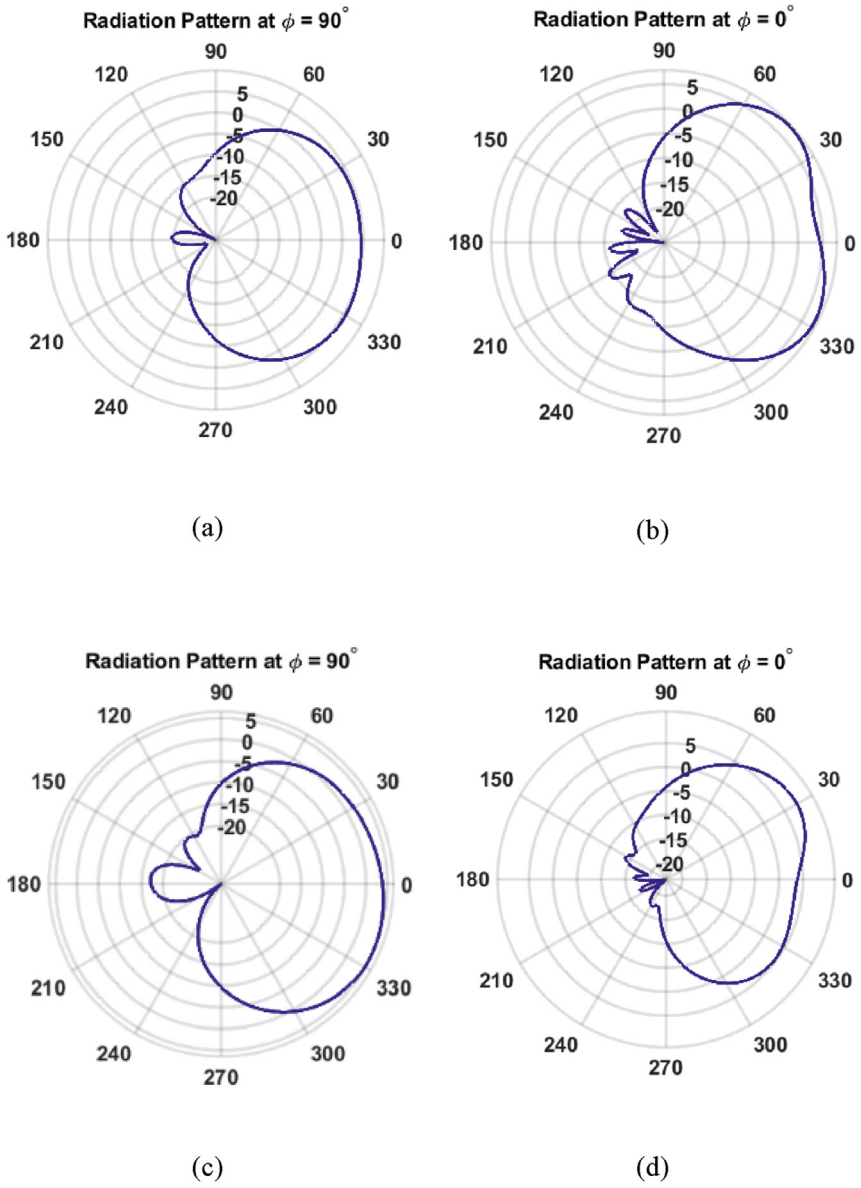

Fig. 11. The simulated radiation pattern of the dual-polarized termination element at 5.3 GHz. (a) −45 slanted polarization at phi = 90°, (b) −45 slanted polarization at phi = 0°, (c) +45 slanted polarization at phi = 90° (d) +45 slanted polarization at phi = 0°.

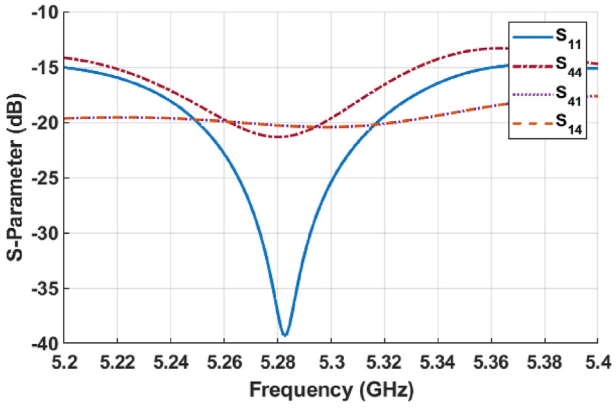

Fig. 12. Simulated S-parameters for the column array.

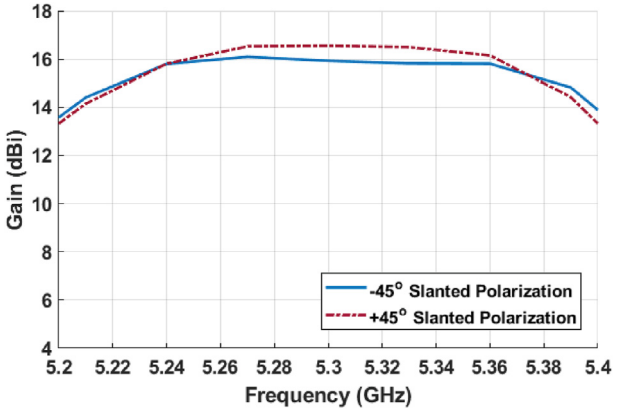

Fig. 13. Simulated gain over frequency of the proposed column array.

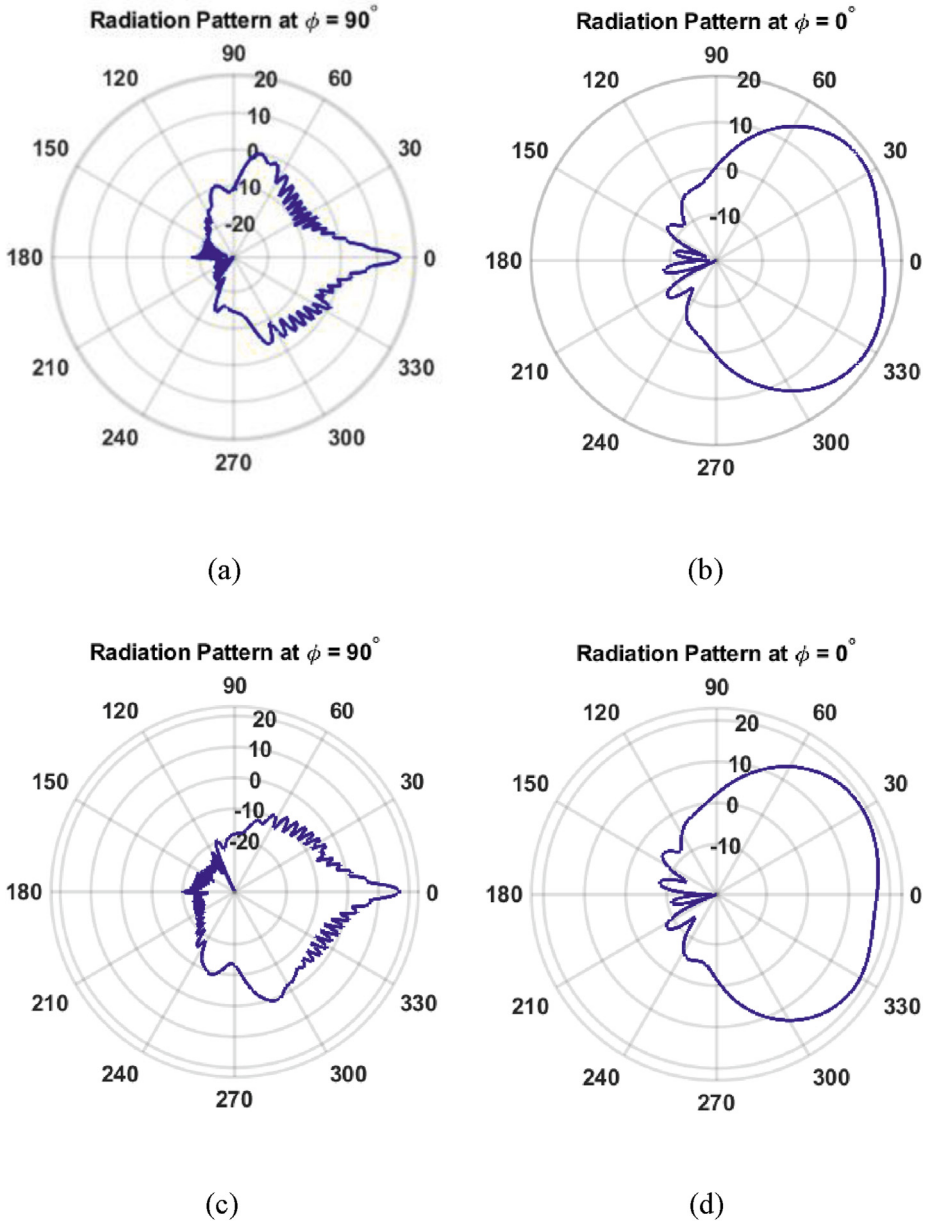

Fig. 14. The simulated radiation pattern of a single column array at 5.3 GHz. (a) −45 slanted polarization at phi = 90°, (b) −45 slanted polarization at phi = 0°, (c) +45 slanted polarization at phi = 90° (d) +45 slanted polarization at phi = 0°.

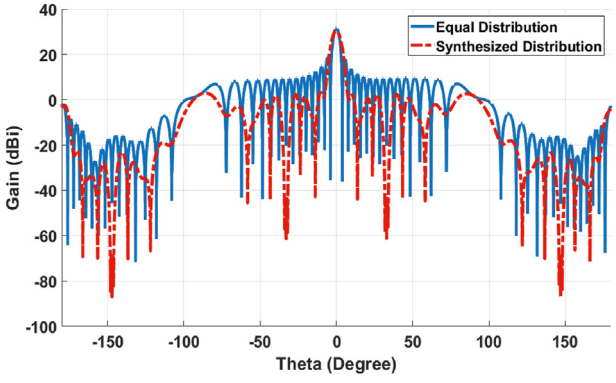

Fig. 15. The difference between the equal distribution and synthesized distribution for the same number of elements.

The proposed antenna is subjected to arbitrary application of the synthesized algorithm, such as MoM/GA. It means arbitrary beam shape, beam width, and SLL can be achieved using the proposed antenna array. To apply the MoM/GA algorithm, a feeding network with specific excitation should be designed. A novel feeding network design is proposed to provide the required excitations with an easy-to-design and fabrication structure.

The proposed structure is a single-layer planar antenna array that is easily fabricated compared to the multilayer arrays (Kashihara et al., 2023; Yu et al., 2020), and the 3D waveguide structure array (Ravindra et al., 2017). The proposed antenna can

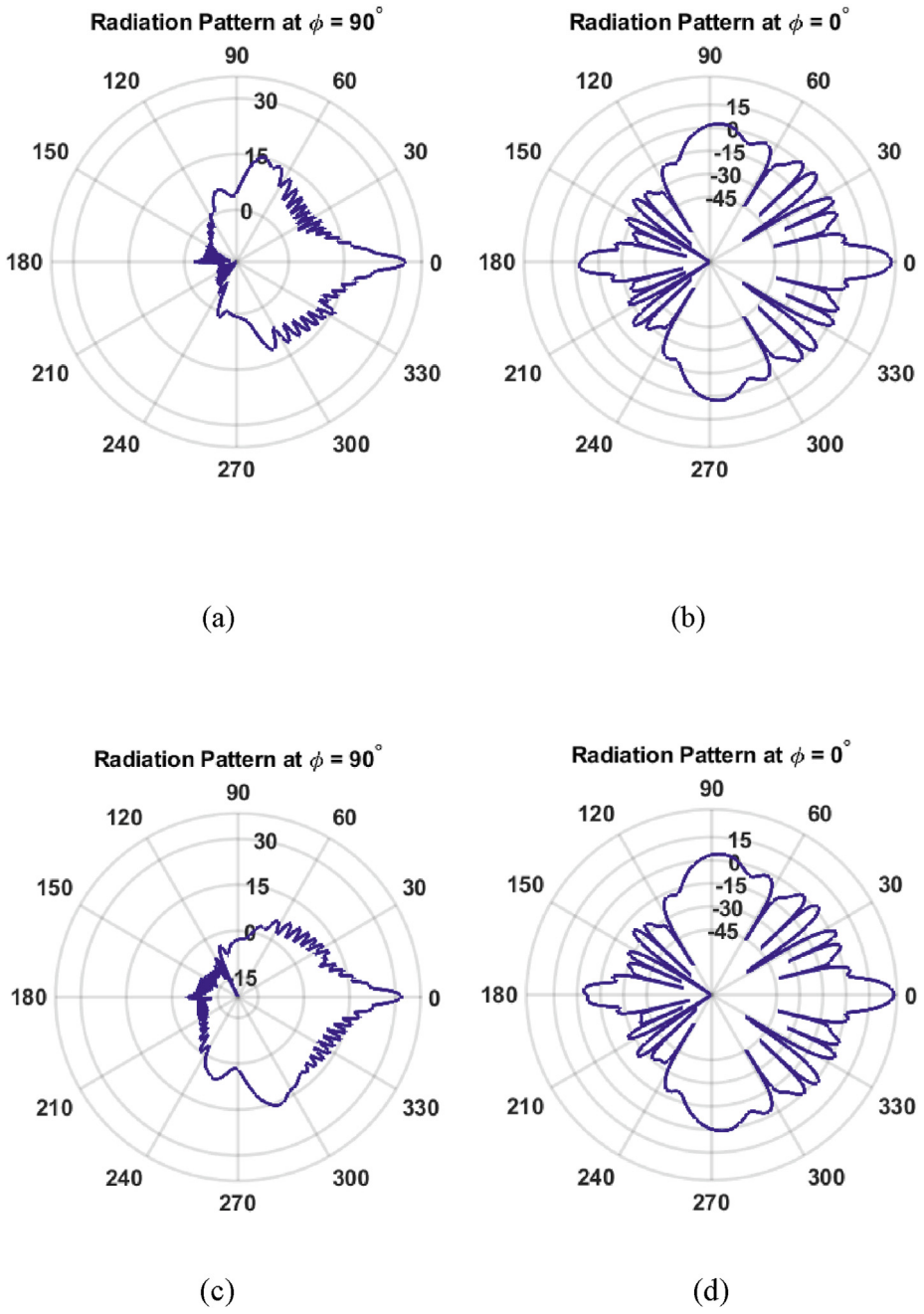

Fig. 16. The simulated radiation pattern of the planar array at 5.3 GHz. (a) −45 slanted polarization at phi = 90°, (b) −45 slanted polarization at phi = 0°, (c) +45 slanted polarization at phi = 90° (d) +45 slanted polarization at phi = 0°.

achieve an approximate similar gain as in (Ravindra et al., 2017), but with smaller dimensions relative to the wavelength and a simpler structure. The antenna should provide dual polarization radiation, in comparison with the linear polarization in (Yu et al., 2020). In (Kashihara et al., 2023), the presented work provides dual circular polarization by duplicating the antenna. It is considered to target an oriented antenna design in contradiction to our proposed work that suits arbitrary beam shapes.

The proposed antenna can achieve a low SLL in the range direction due to the use of the MoM/GA synthesized coefficients compared to previous works. Due to its larger structure, the array in (Ravindra et al., 2017) provides a smaller beamwidth of 2.4° in the azimuth and range planes compared to 5.1° in the azimuth plane and 4.2° in the range plane in the proposed work.

The proposed work achieves a high gain of 30 dBi with an exceptionally low SLL of −27.2 dB in the

Table 6. Performance comparison between the proposed SAR antenna and reported ones.

Ref	Bandwidth (GHz)	Dimensions (cm^3)	Range HPBW	Azimuth HPBW	Range SLL	Azimuth SLL	Gain	Polarization	Feeding technique
Yu et al. (2020)	21–29	6.25λ x 7.5λ x 0.1λ	15°	9°	−15 dB	−15 dB	20.4 dBi	Linear	Series + Corporate
Kashihara et al. (2023)	8.8–10.2	3.6λ x 3.6λ x 0.11λ	15°	15°	−13 dB	−13 dB	21.6 dBi	Dual Circular	Corporate Feed
Ravindra et al. (2017)	9.5:9.8	22.6λ x 22.6λ x 0.55λ	2.4°	2.4°	−15 dB	−11 dB	34.5 dBic	Dual Circular	Waveguide
Proposed	5.2–5.4	14.9λ x 14.1λ x 0.014λ	5.1°	4.2°	−27.2 dB	−12.7 dB	30 dBi	Dual Linear	Series + Corporate

range direction. The proposed antenna can also produce a dual-linear polarization, which is needed to improve the resolution of the sensor. The proposed design achieves narrow beam widths of 5.1° and 4.2° in range and azimuth directions, respectively. The antenna array has a simple design with a very low profile, which reduces the fabrication and integration challenges. Also, fabricating the overall antenna on a single substrate improves the antenna's reliability and efficiency. The SLL in the azimuth direction is −12.7 dB, which is not as good as some of the reported investigations, and it can be improved by applying a different field distribution across the linear array.

4. Conclusions

A synthesized planar antenna array with low SLL, high gain, and capable of radiating with dual linear polarizations has been proposed for C-band spaceborne SAR applications. The array is composed of 16 × 18 antenna elements. The proposed array uses the series feed technique to connect the linear column arrays and the corporate feed to form the planar array. The series feed technique reduces the loss generated by a large feeding network. And the corporate feeding technique provides flexibility in designing an array with specific excitation values, which can improve the SLL. By merging the features provided by the two feeding techniques and building the overall antenna on a single substrate, the efficiency, gain, and SLL of the antenna are enhanced, which enhances the capability of the sensor. The MoM/GA algorithm is used to generate a synthesized field distribution across the planar array, which enhances the SLL. The drawback with the MoM/GA is that it produces excitations that cannot be easily applied. To overcome this problem, A novel feeding network design is proposed to obtain the required excitations without the use of power dividers with high dividing ratios. The designed feeding network provides the same required excitations but narrows the large gap between the dividing ratios, which makes it more applicable. The proposed design simplifies the design of the feeding network and therefore the overall antenna. The antenna achieves a $|S11|<-10$ dB bandwidth from 5.2 GHz to 5.4 GHz, an HPBW of 4.2° in the range direction, 5.1° in the azimuth direction, and a peak gain of 30 dBi. The SLL is −12.7 dB and −27.2 dB in azimuth and range directions, respectively. In future work, the SLL in the azimuth direction needs more improvement; this can be done by controlling the field distributions for each element in the column array.

Author credit statement

Ahmed E. Gohar: Conception and design of the work, data collection and tools, data analysis, methodology, reporting and plotting the results, and drafting of the article. *Haythem H. Abdullah*: Conception and design of the work, Supervision, project management, methodology, resources, and critical revision of the article. *Mohy El din Abo Elsoud*: Supervision, and final approval of the version to be published.

Funding statement

The author did not receive any financial support for the research authorship and publication of this article.

Conflict of interest

There are no conflicts of interest.

Acknowledgements

This work was supported in part by the Egyptian Space Agency (EgSA), and in part by the Electronics Research Institute (ERI), Egypt, in the project entitled SAR Sensor Design.

References

Bayderkhani, R., Hassani, H.R., 2010. Wideband and low sidelobe slot antenna fed by series-fed printed array. IEEE Trans.

Antenn. Propag. 58, 3898–3904. https://doi.org/10.1109/TAP.2010.2078437.
Corporation R. Low Outgassing Characteristics of Rogers Laminates Approved for Spacecraft Applications p. 2.
Eldosouky, B., Hussein, A., Abdullah, H., Khamis, S., Nov. 2013. Synthesis of Pencil Beam Linear Antenna Arrays Using Simple FFT/CF/GA Based Technique, vol. 13.
Harrington, R.F., 1993. Field Computation by Moment Methods, Reprint edition. Wiley-IEEE Press, Piscataway, NJ.
Haupt, R.L., Werner, D.H., 2010. Genetic Algorithms in Electromagnetics, first ed. Wiley-IEEE Press, Piscataway, NJ.
Hussein, A.H., Abdullah, H.H., Salem, A.M., Khamis, S., Nasr, M., 2011. Optimum design of linear antenna arrays using a hybrid MoM/GA algorithm. IEEE Antenn. Wireless Propag. Lett. 10, 1232–1235. https://doi.org/10.1109/LAWP.2011.2174189.
Kashihara, H., Sumantyo, J.T.S., Izumi, Y., Ito, K., Gao, S., Namba, K., 2023. X-band microstrip array antenna for UAV onboard full circularly polarized synthetic aperture radar. IEEE Trans. Antenn. Propag. 71, 1943–1948. https://doi.org/10.1109/TAP.2022.3232745.
Li, Y., Zhang, Z., Feng, Z., Iskander, M.F., 2011. Dual-mode loop antenna with compact feed for polarization diversity. IEEE Antenn. Wireless Propag. Lett. 10, 95–98. https://doi.org/10.1109/LAWP.2011.2112752.
Li, Y., Zhang, Z., Deng, C., Feng, Z., Iskander, M.F., 2014. 2-D planar scalable dual-polarized series-fed slot antenna array using single substrate. IEEE Trans. Antenn. Propag. 62, 2280–2283. https://doi.org/10.1109/TAP.2014.2300178.
Lv, Y., Shen, D., Ren, W., He, J., Zeng, J., 2015. 'An equal-split Wilkinson power divider with tri-band and harmonic suppression. In: 2015 IEEE International Wireless Symposium (IWS 2015), pp. 1–4, Shenzhen, China. https://doi.org/10.1109/IEEE-IWS.2015.7164604.
Metzler, T., 1981. Microstrip series arrays. IEEE Trans. Antenn. Propag. 29, 174–178. https://doi.org/10.1109/TAP.1981.1142543.
Pozar, D.M., Schaubert, D.H., Jun. 1993. Comparison of three series fed microstrip array geometries. In: Proceedings of IEEE Antennas and Propagation Society International Symposium, vol. 2, pp. 728–731, Ann Arbor, MI, USA. https://doi.org/10.1109/APS.1993.385244.
Qin, F., Gao, S.S., Luo, Q., Mao, C.X., Gu, C., Wei, G., et al., 2016. A Simple low-cost shared-aperture dual-band dual-polarized high-gain antenna for synthetic aperture radars. IEEE Trans. Antenn. Propag. 64, 2914–2922. https://doi.org/10.1109/TAP.2016.2559526.
Rahmat-Samii, Y., Michielssen, E. (Eds.), 1999. Electromagnetic Optimization by Genetic Algorithms, first ed. Wiley-Interscience, New York.
Ravindra, V., Akbar, P.R., Zhang, M., Hirokawa, J., Saito, H., Oyama, A., 2017. A dual-polarization X -band traveling-wave antenna panel for small-satellite synthetic aperture radar. IEEE Trans. Antenn. Propag. 65, 2144–2156. https://doi.org/10.1109/TAP.2017.2676760.
Riyazuddin, M., Bharath, J.R., 2015. Design and simulation of C-band microstrip corporate feed array antenna. In: 2015 13th International Conference on Electromagnetic Interference and Compatibility (INCEMIC), pp. 182–186, Visakhapatnam, India. https://doi.org/10.1109/INCEMIC.2015.8055876.
Santosa, C.E., Sumantyo, J.T.S., Gao, S., Ito, K., 2021. Broadband circularly polarized microstrip array antenna with curved-truncation and circle-slotted Parasitic. IEEE Trans. Antenn. Propag. 69, 5524–5533. https://doi.org/10.1109/TAP.2021.3060122.
Vallecchi, A., Gentili, G.B., 2005. Design of dual-polarized series-fed microstrip arrays with low losses and high polarization purity. IEEE Trans. Antenn. Propag. 53, 1791–1798. https://doi.org/10.1109/TAP.2005.846732.
Wang, C.-J., Chen, L.-T., Feb. 2014. Modeling of stepped-impedance slot antenna. IEEE Trans. Antenn. Propag. 62, 955–959. https://doi.org/10.1109/TAP.2013.2291906.
Weily, A.R., Guo, Y.J., 2009. Circularly polarized ellipse-loaded circular slot array for millimeter-wave WPAN applications. IEEE Trans. Antenn. Propag. 57, 2862–2870. https://doi.org/10.1109/TAP.2009.2029305.
Yu, Y., Jiang, Z.H., Zhang, H., Zhang, Z., Hong, W., 2020. A low-profile beamforming patch array with a cosecant fourth power pattern for millimeter-wave synthetic aperture radar applications. IEEE Trans. Antenn. Propag. 68, 6486–6496. https://doi.org/10.1109/TAP.2020.2999669.
Zhou, W.-L., Qu, S.-W., Xia, M., Yang, S., 2022. Wideband L/X-band shared-aperture phased array antenna for SAR applications. IEEE Trans. Antenn. Propag. 70, 10475–10484. https://doi.org/10.1109/TAP.2022.3195454.